Sedimentary Geology 230 (2010) 46–59

Contents lists available at ScienceDirect

Sedimentary Geology

journal homepage: www.elsevier.com/locate/sedgeo

Sand injectites at the base of the Coconino Sandstone, Grand Canyon, Arizona (USA)

John H. Whitmore [a,*], Ray Strom [b,1]

[a] Cedarville University, 251 N. Main St., Cedarville, Ohio 45314 USA
[b] Calgary Rock and Materials Services, Inc., #3, 3610-29th St. NE, Calgary, Alberta, Canada T1Y 5Z7

ARTICLE INFO

Article history:
Received 24 September 2009
Received in revised form 24 June 2010
Accepted 25 June 2010
Available online 31 July 2010

Editor: G.J. Weltje

Keywords:
Sand injectites
Clastic dikes
Desiccation cracks
Coconino Sandstone
Seismites
Mud cracks

ABSTRACT

In the Grand Canyon, large tabular and wedge shaped sand-filled cracks commonly occur at the base of the Coconino Sandstone, penetrating downward into the coarse siltstones of the Hermit Formation. All previous workers have casually identified the vertical sand-filled cracks as desiccation cracks. Until now, they have never been studied. Cracks and their associated features were found and examined at thirty locations; and it was found that they have characteristics difficult to explain using desiccation mud cracks or large playa cracks as a model. Instead, it was found the cracks have features commonly found in clastic dikes and sand injectites. Some lateral sand bodies associated with the cracks have clastic sill-like characteristics. Liquefaction and injection of the basal Coconino into the Hermit is indicated by 1) macroscopic and microscopic banding (flow structures) within the cracks, 2) bedded sandstone clast breccias in structureless sandstone lenses at the base of the Coconino, 3) lateral sand bodies which are connected to the vertical cracks, 4) a zoned depth distribution of cracks about the Bright Angel Fault zone, 5) insufficient clay mineralogy and particle size for the Hermit to crack by desiccation, 6) preferred orientation of the cracks roughly perpendicular to the Bright Angel Fault zone and several other features. Caution should be exercised when interpreting sand-filled cracks as desiccation features (i.e., "mud cracks"), even if the interpretation fits well with accepted paleoenvironmental models.

1. Introduction

Large tabular and wedge shaped sand-filled cracks can often be found at the base of the Coconino Sandstone penetrating vertically and sometimes horizontally into the mudstones of the Hermit Formation. The deepest known cracks occur along the Bright Angel Trail near Grand Canyon Village in Arizona. Some cracks are at least 15 m deep and 0.25 m wide (Fig. 1). They have been identified as desiccation cracks in the popular and scientific literature (White, 1929; McKee, 1934; Abbott and Cook, 2004) probably because of the fluvial and coastal plain environment favored for the red beds of the Hermit (Blakey, 1990), the eolian interpretation for the overlying Coconino (McKee, 1934, 1979; Blakey, 1996) and the tabular or wedge shaped pattern expected of desiccation cracks. Although known for at least 88 years (Noble, 1922), the cracks have never been extensively studied or described with the exception of White's (1929) single petrographic photo and brief comment. Several features of the cracks make their interpretation as desiccation cracks doubtful. These observations include the wrong clay mineralogy and particle size for the Hermit to crack via desiccation, cracks within the Hermit that taper upward and are not directly connected to the Coconino, vertical lineations found within many of the cracks and lateral sand bodies connected to some of the cracks. No one has reported this last fact, which may help explain McKee's puzzling observation (1934, p. 87) that there are "pockets" of the Coconino Sandstone near the top of the Hermit along Hance Trail. We think, based on associated features, the vertical cracks represent injected clastic dikes and the horizontal sand bodies may represent clastic sills, probably of seismic origin.

It is not uncommon for well established examples of desiccation cracks to be questioned or even reinterpreted (Donovan and Foster, 1972; Plummer and Gostin, 1981; Astin and Rogers, 1991; Cowan and James, 1992; Barclay et al., 1993; Pratt, 1998a,b) because of their similarity to other types of sand-filled cracks. Extreme caution should be exercised when interpreting all types of sand-filled cracks (mud cracks, synaeresis cracks, diastasis cracks, molar tooth structures, etc.) because of the similar features they share. Paleoenvironmental presuppositions can lead to erroneous interpretations of various features and might cause one to overlook important data. In this case, the cracks have never been examined closely because mud cracks are expected on desiccating mudflats, which is the accepted paleoenvironment of the Hermit. Subsequently, many important features of the cracks have never been recognized and their true origin has remained hidden.

* Corresponding author. Fax: +1 937 766 7631.
E-mail addresses: johnwhitmore@cedarville.edu (J.H. Whitmore), rocktell@telus.net (R. Strom).
[1] Fax: +1 403 735 5058.

0037-0738/$ – see front matter © 2010 Elsevier B.V. All rights reserved.
doi:10.1016/j.sedgeo.2010.06.022

2. Methods and observations

2.1. Description of the sand-filled cracks

The Hermit/Coconino contact was visited at thirty-six locations in and around the Grand Canyon (Fig. 2, Table 1) so the broad extent of the cracks could be determined. Where hiking trails were not present, sand-filled cracks were observed with a telescope. At each trail location major cracks were numbered, measured, described and photographed (numbering more than 75 major cracks). At overlook locations, the presence, the relative number (few, many), and the depth of cracks (<1 m, ~1 m, >1 m) were estimated and recorded. Samples were collected from two sites within Grand Canyon National Park (SK and NH, permit # GRCA-2005-SCI-0011) and several sites outside of the park for thin section analysis. In all, ten different cracks from five different locations were sampled and studied petrographically. The samples were of sufficient size to make multiple petrographic slides of each sample collected, including different orientations. All of the sand-filled cracks sampled were from what have typically been called "mud cracks." Samples of the Hermit were also collected at several locations (at sites with and without cracks) for thin section and XRD analysis. Sample preparation and analysis was completed at Calgary Rock and Materials Services Inc., in Alberta.

The largest average crack depths occur in the vicinity of the Bright Angel Trail (>8.7 m). This is adjacent to the greatest displacement (61 m in the Permian rocks) of the northeast trending Bright Angel Fault (Huntoon et al. (1996) report 200 feet on their map). The fault is normal and dips steeply (85°) at the surface and then shallows at depth (to about 45°) causing reverse drag in the Paleozoic rocks (Huntoon and Sears, 1975). Average crack depths become shallower to the east and west, disappearing altogether along Tanner and South Bass Trails. McKee (1934, p. 86) shows a similar pattern of crack depths along the South Rim in his Coconino monograph (Fig. 3). Along the Bright Angel Fault on the north side of the Grand Canyon, where the displacement of the fault is less (15 m in the Permian rocks), we found cracks were still present but they are on average much shallower (1.2 m on North Kaibab and ~1 m further to the north at Vista Encantada). To the west, cracks are shallow or absent along Bill Hall Trail and Thunder River Trails. No cracks were found at places outside the map area (Fig. 2) including Andrus Canyon, Parashant Canyon, Whitmore Canyon, Hurricane Cliffs and near the towns of Show Low, Sedona, Seligman, Drake and Pine, Arizona. When found, cracks are variable in depths at all locations. For example, at Bright Angel Trail nine major cracks were measured having minimum vertical dimensions of 2, 10, 12, 15, 10, 2, 2, 10 and 15 m. Deep (>1 m) and thick (~10 cm) vertical cracks are never widely spaced (Fig. 4G); one usually occurring between 2 and 15 m at all locations (0.5–0.06 cracks per m).

Many of the cracks are deep and narrow (Fig. 1). However, several were found that tapered upward (Fig. 4A), some are "U" shaped (Fig. 4B), several cut directly through sand bodies within the Hermit (Fig. 4C), several appeared suddenly without any obvious connections to the Coconino (Fig. 4D), and some penetrated at a downward angle into the Hermit (Fig. 4E). Sometimes shallower and narrower cracks exhibit ptygmatic folds; deeper and larger cracks are usually planar. Most cracks are structureless in appearance and do not contain any obvious bedding, banding or layering. However, several cracks at each location usually contain vertical lineations or banding, parallel to crack walls (Figs. 4F, 5A, D, G). One thin section (of crack HN1) showed horizontal lineations within cracks, similar in scale and structure to the vertical lineations, although we never found this macroscopically. Macroscopic clasts of Hermit mudstone can occasionally be found in cracks, usually a few millimeters in diameter. The clasts are not common. All clasts were in a matrix of Coconino-like sand. Some large pieces of Hermit were found in several locations that were completely surrounded in a matrix of sand (see inset in Fig. 4C). Slickenside-like features (Fig. 6), which were different from the vertical lineations, are found within some of the cracks along the Bright Angel Trail and Jumpup Spring. The structures are sub-vertical, cutting through the cracks at an angle. No obvious offset was observed within the cracks, the surrounding Hermit, or the Coconino, so the features cannot be true slickensides, although they bore the striated and polished resemblance of slickensides. Thin section analysis of "slickensides" from Jumpup Spring showed calcite mineralization where the features occurred. The underside of the Coconino was examined at all possible locations in search of multiple generations (orders) of cracks that are typically found on modern mud cracked surfaces. No convincing evidence of multiple crack orders was found.

At several locations, cracks intersect with each other. At the Bright Angel location, an upslope view of two large intersecting cracks can be observed (Fig. 1). No cross cutting relationships at the crack intersection was obvious. Junctions of cracks were observed at several locations. Sixty-eight different cracks from nine locations were exposed in such a way that their orientations (strike) could be measured. All of the cracks had vertical, or near vertical dips. Dip was not measured. A rose diagram of the strike data is presented in the top corner of Fig. 2. The mean vector (μ) of the cracks was 142.8º, with the 95% confidence interval for the mean between 126.6° and 159.1°. Statistical tests for circular data in the software package showed the cracks were probably not randomly oriented. The Rayleigh Test had a ρ value of 0.003 and Rao's Spacing Test also gave a ρ value of <0.05. The rose diagram and statistics were plotted and calculated using *Oriana v. 3.13* software, copyright © 1994–2010 Kovach Computing Services.

Fig. 1. Two intersecting sand-filled cracks near the Bright Angel Trail, Grand Canyon. One crack is coming toward the viewer (white arrows) and another crack is intersecting the first (black arrows). Each crack is about 20 cm wide and they penetrate at least 10–15 m into the Hermit (the bottoms of the cracks were buried). The base of the Coconino Sandstone is at the tip of the upper white arrow.

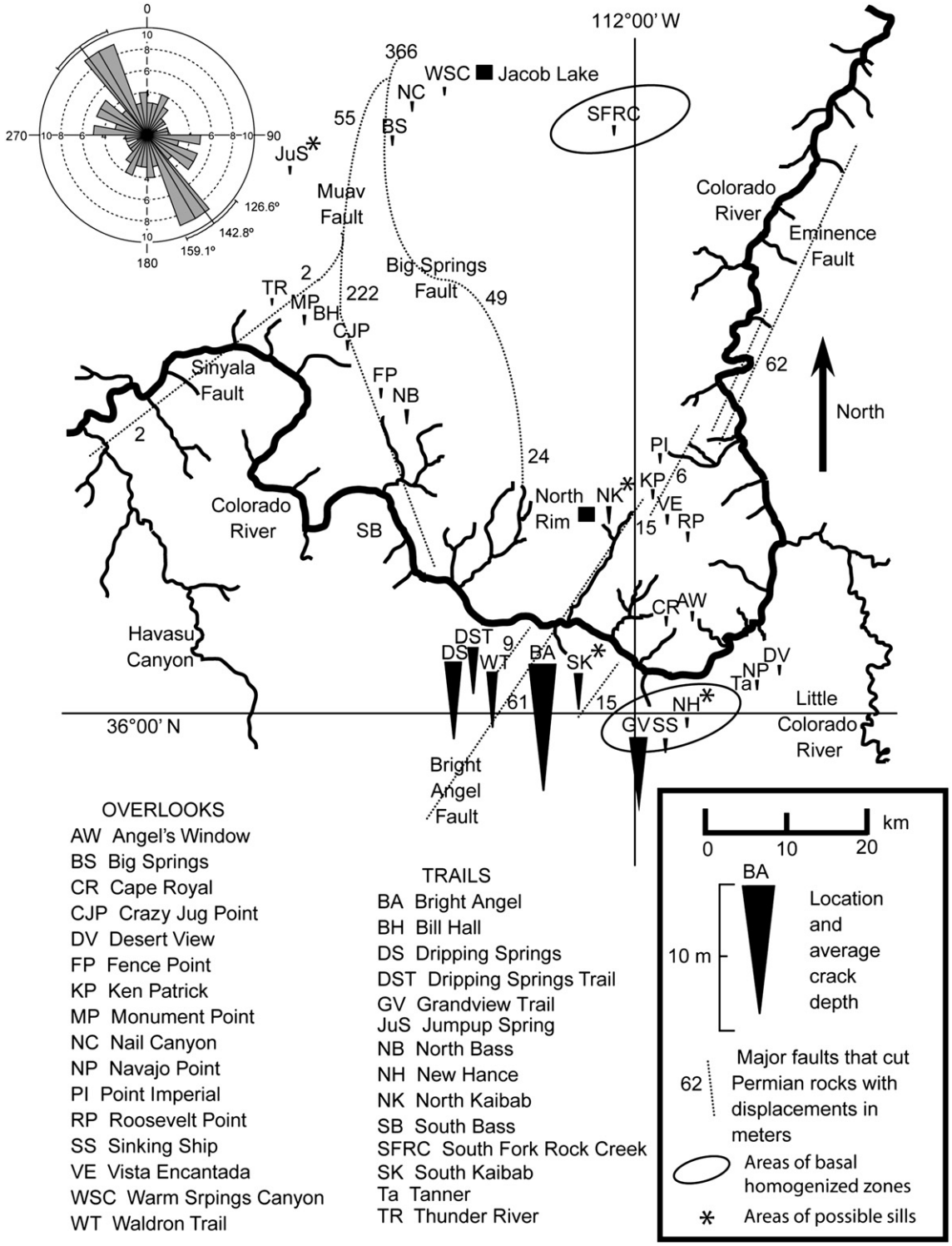

Fig. 2. Sand-filled crack observations at overlooks and trails in the Grand Canyon region, Arizona. Wedge height represents average crack depth. See Table 1 for details. Some locations are not listed on the map because no cracks were present and they were out of the map area (see text). The inset in the upper left corner of the map shows sand-filled crack orientation statistics. Nine sites had cracks with measureable orientations (n = 68): BA (n = 7), DS (n = 9), JuS (n = 7), NB (n = 4), NH (n = 12), NK (n = 10), SFRC (n = 9), SK (n = 5) and TR (n = 5). All the cracks had vertical or near vertical dips. The rose diagram petal width is 10°. The mean vector (μ) is 142.8°; the circular standard deviation is 45.1°; the standard error of mean is 8.3°; and the 95% confidence interval (+/−) for the mean is 126.6 to 159.1°. The Bright Angel and Eminence Faults are steeply dipping normal faults. Many minor faults are not shown.

Petrographic analysis of the cracks and the Coconino Sandstone (Tables 2 and 3) found the cracks were mostly filled with quartz sand, similar to Coconino sand (see Fig. 5). Petrographic analysis confirmed the presence of vertical "flow structures" within many of the cracks. Porosity values were noticeably higher in typical cross-bedded Coconino Sandstone compared to the structureless (or homogenized) zone at the base of the Coconino and the sand-filled cracks. Respective porosity values were approximately 15, 8 and 4%. Petrographic

Table 1
Sand-filled crack depths, Grand Canyon and vicinity, Arizona.

Location	Number of major cracks	Deepest crack (m)	Average major crack depth (m)
Andrus Canyon (AC) (w. of map area)	Absent	–	–
Andrus Point (AP) (w. of map area)	Absent	–	–
Angel's Window Overlook (AW)	Few	<1	<1
Bill Hall Trail (BH)	Absent	–	–
Big Springs (BS)	Many	~1	<1
Bright Angel Trail (BA)	9	>15	>8.7
Cape Royal Overlook (CR)	Few	<1	<1
Crazy Jug Point Overlook (CJP)	Few	<1	<1
Desert View Overlook (DV)	Few	<1	<1
Dripping Springs (DS)	10	>10	>5.3
Dripping Springs Trail (DST)	4	>6	>3.2
Fence Point Overlook (FP)	Few	<1	<1
Grandview Trail (GV)	Few	6	~5
Hurricane Cliffs (HC) (nw of map)	Absent	–	–
Jumpup Spring (JuS)	8	1.5	0.7
Ken Patrick Overlook (KP)	Few	~1	<1
Monument Point Overlook (MP)	Few	<1	<1
Nail Canyon (NC)	Many	>1	<1
Navajo Point Overlook (NP)	Few	<1	<1
New Hance Trail (NH)	8	1.2	0.7
North Bass Trail (NB)	5	1.5	1.0
North Kaibab Trail (NK)	10	2.0	1.2
Parashant Canyon (w. of map area)	Absent	–	–
Point Imperial Overlook (PI)	Few	~1	<1
Roosevelt Point Overlook (RP)	Few	<1	<1
Sinking Ship Overlook (SS)	Many	>1	~1
South Bass Trail (SB)	Absent	–	–
South Fork Rock Canyon(SFRC)	10	1.8	0.9
South Kaibab Trail (SK)	7	4.5	2.5
Tanner Trail (Ta)	Absent	–	–
Trail Canyon (TC) (w. of map area)	Absent	–	–
Thunder River Trail (TR)	5	1.0	0.5
Vista Encantada Overlook (VE)	Few	>1	~1
Waldron Trail (overlook)	Many	6?	3?
Warm Springs Canyon (WSC)	Many	>1	<1
Whitmore Canyon (WC) (w. of map)	Absent	–	–

At "overlook" locations a spotting scope was used to estimate crack depth and abundance. At "trail" locations crack depth was measured directly.

observation of sand grains within the sand-filled cracks showed marked evidence of compaction and distortion compared to the normal cross-bedded Coconino.

2.2. Description of lateral sand bodies within the Hermit associated with the cracks

Lateral sand bodies which have Coconino-like lithologies are clearly associated with the vertical sand-filled cracks along New Hance Trail (hereafter called "Hance Trail"), at Jumpup Spring and along North and South Kaibab Trails. The lateral sand bodies are not common, and usually not very large, compared to the vertical sand-filled cracks. At both of the Kaibab Trail locations, narrow sand-filled cracks can be found that clearly penetrate all the way through the lateral, 10–20 cm thick sand bodies (Fig. 4C). At Hance Trail, several larger lateral sand bodies were found These probably represent McKee's "pockets of Coconino" that he described near the top of the Hermit (1934, p. 87). The bodies are lens shaped, 1–2 m thick and about 25 m long (Fig. 7). At the distal ends of the bodies, distorted Hermit bedding can be found around the body, perhaps due to the

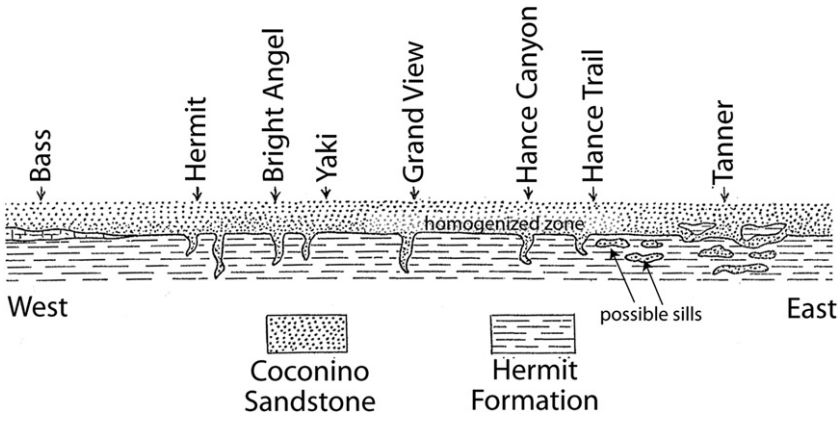

Fig. 3. McKee's drawing (1934, p. 86) showing sand-filled crack depths along the South Rim of the Grand Canyon. McKee's data is consistent with our own; showing deeper cracks in the vicinity of the Bright Angel Fault (see Fig. 2). The figure shows the location of the homogenized zone we found and the location of possible clastic sills in the vicinity of the Hance Trail. At Tanner Trail, McKee shows that the contact between the Hermit and Coconino is a transitional one; a fact which we confirmed in the field.

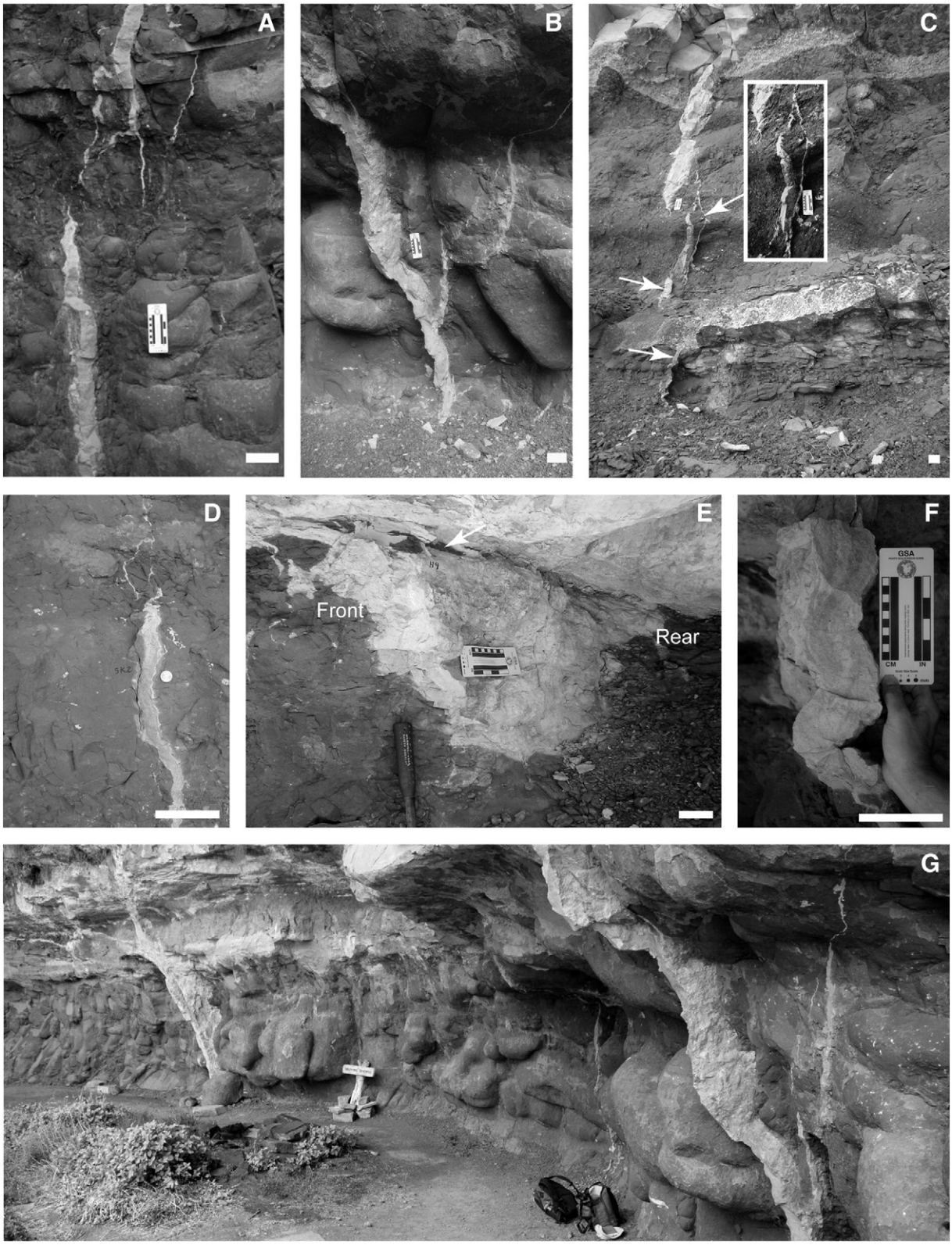

Fig. 4. Major differences between the sand-filled cracks in the Grand Canyon and desiccation mud cracks. A: Some taper upward (DS1). B: Some are "U" shaped (DS7). The orientation into the outcrop of the crack on the right and the crack on the left is about 60° different. C: Some penetrate through horizontal sand bodies within the Hermit (SK3). The lower two arrows show the crack just above and below the sand body. The inset shows a large piece of Hermit completely surrounded by narrow sand-filled cracks. If these were mud cracks, it would be difficult to understand how the cracks could rejoin below the large piece of Hermit they surround. This cannot be mud crack fill because the Hermit is surrounded on all sides by sand. D: Some appear suddenly without any obvious connection to the Coconino (SK2). E: Some penetrate at a downward angle into the Hermit. Note that some of the Hermit Formation occurs on top of the crack near the front (at arrow), but disappears toward the rear of the crack, where the crack is connected to the Coconino (NH4). F: Some appear to have vertical flow structures or banding (NH3). G: The cracks are more narrowly spaced than playa cracks (DS). Note back packs for scale in bottom center of picture. Crack DS7 is closest to the right. Each scale bar is 10 cm long (lower right of A–F). Location and crack number in parentheses.

forceful injection of sand (Fig. 8). The sand body at Jumpup Spring is small, but is directly connected to a vertical sand-filled crack (about 55 cm deep), which in turn is connected to the Coconino above. Here, the sand body is about 70 cm long and about 10 cm wide.

2.3. The basal Coconino homogenized zone and other features

Bedding is easily distinguished throughout the Coconino, but along Hance Trail, Grandview Trail and the South Fork of Rock Canyon, lenses of non-bedded structureless sandstone, up to 2.0 meters thick and 40 m long, rest on the Hermit at the base of the Coconino (Figs. 9–11). The zones are continuous and intimately connected with sand-filled cracks (Figs. 4E and 10). The Coconino bedding and cross-bedding in contact with the structureless sandstone, or homogenized zone, can occur as a sharp contact (Fig. 9), or as distorted bedding grading upward into "normal" Coconino cross-beds (right center of Fig. 11). The homogenized zone occasionally contains bedded Coconino clasts, with long axes from 2 to 75 cm (Figs. 9 and 11). Bedding angles inside the clasts are often askew. Along Hance Trail, features similar to load casts occur at the base of the Coconino. These features are intimately associated with dozens of shallow, distorted sand-filled cracks and the homogenized sandstone. The smaller casts (Fig. 12) are about 8–10 cm in diameter. One larger cast was found that was about 50 cm in diameter. It was also directly associated with a large sand-filled crack.

2.4. XRD analysis of the Hermit Formation, Lucerne Dry Lake and other cracked playas

XRD and petrographic analysis of the Hermit Formation next to the cracks, and in locations where the cracks did not occur, showed a consistent composition of very fine grained sand and coarse silt for the Hermit (a grain size average of about 55 μm). The Hermit contained less than 3% clay minerals and less than 5.5% clay sized particles at all locations analyzed (Table 4). For comparison, Lucerne Dry Lake, California, contained 25.9% clay sized particles and about 9% (by volume) clay minerals. Illite and kaolinite were the dominate clays present in all of the samples tested. Lucerne Dry Lake sediments appear to be slightly coarser than the results reported from 11 other cracked playas by Neal et al. (1968). We report their results in Table 5.

2.5. Playa cracks at Lucerne Dry Lake

Large desiccation playa cracks occur in many dry lake beds (Lang, 1943; Wilden and Mabey, 1961; Neal et al., 1968). We observed them on the ground and from aerial photographs at Lucerne Lake in southern California (Figs. 13 and 14). They form large polygons (about 20–250 m in diameter) with highly variable crack widths (an average of ~1 m) and unknown depths. Crack widths vary because they are filled with material that sloughs from crack walls. Sloughing wall material was commonly observed to completely fill cracks. Filling probably also occurs by wind-blown sand and fluvial processes. Some cracks act as stream channels; others were damp as though they recently had standing water in them. Fill material was excavated and was found to consist of finely laminated muds. Sloughed areas were not excavated, but would likely contain chaotic crack fill interspersed with laminated muds. Ground and aerial observations showed vegetation growing in many of the cracks. The playa surface also contained multiple orders of smaller cracks, some inside the larger ones (Fig. 13). Measurements from aerial photos showed a range between 12 and 40 large cracks along a straight line per km (0.012–0.04 cracks per m) with a mean of about 20 cracks per km (0.02 cracks per m). The large desiccation cracks on Lucerne Dry Lake are about an order of magnitude further apart than the large cracks in Grand Canyon.

3. Discussion

3.1. Desiccation cracks?

It appears the Hermit has the wrong clay mineralogy and lithology for the cracks to be explained via desiccation. It is not rich in clay minerals or clay-sized particles that are required for desiccation cracking (Table 4). Modern soils that crack via desiccation have significantly more clay than does the Hermit. Yassoglou et al. (1994), Basma et al. (1996), Yesiller et al. (2000), and Harianto et al. (2008) report cracking in soils with clay contents ranging from 13 to 58.3% and silt contents ranging from 21 to 52%. Lucerne Dry Lake had 9% clay minerals by volume and 25.9% clay sized particles by mass. Neal et al. (1968) reported clay analyses from 11 of the 39 playas they studied with giant desiccation cracks (Table 5). They observed (p. 81) that "particle-size measurements in giant-fissured playa areas indicate that sediments contain substantial amounts of <5 μm material." In their samples, kaolinite was usually absent from playa fissured surfaces. They state (p. 80): "The clay assemblage of the polygonal cracked areas, as well as other fissured clay playas, is made up primarily of illite, montmorillonite, vermiculite, and chlorite. Little or no kaolinite has been detected in any sample." Kaolinite is the second most abundant clay in the Hermit comprising from 12 to 40% of the clay minerals. The largest fraction of clay minerals found in the Hermit was 3% at WC (no cracks present) and the largest fraction of clay particles found in the Hermit was 5.5% at WSC (which had some small cracks). From our analysis, it does not appear the Hermit has enough clay sized particles, the necessary percentage of clay minerals, or the right combination of clay minerals to crack via desiccation. The Hermit is not comparable to modern playa cracked surfaces.

The sand-filled cracks at the base of the Coconino differ greatly from smaller desiccation cracks and larger playa cracks. No horizontal bedding, evidence of fluvial activity or sloughing of the Hermit was observed in the Grand Canyon cracks. Large sloughed pieces of Hermit were not found in the cracks, as might be expected from the observations made at Lucerne Lake. Instead, many of the cracks have vertical flow structures (or banding) within them, similar to other clastic dikes and injectites (Jenkins, 1925a; Harms, 1965; Peterson, 1968; Scott et al., 2009). Jenkins (1925b) showed experimentally how vertical flow structures are developed within downward injected clastic dikes. The structures we found are similar to those that Jenkins produced experimentally. The crack fill often contains rounded pieces of Hermit clast material (see Fig. 5). The clasts are matrix supported, which can originate in fluid mass flow processes. The small entrained granules of Hermit are much smaller than the large sloughed sides of playa cracks we observed at Lucerne Lake. Even the largest Grand Canyon cracks (~0.25 m wide) are much narrower than most of those observed on Lucerne Lake (~0.75 m wide) and other areas where large ground fissures have developed due to desiccation (Neal et al., 1968; Harris, 2004).

Other differences with the Grand Canyon cracks and observed desiccation cracks include: 1) non-uniform depth at any one location; 2) some taper upward (Fig. 4A, D); 3) some are "U" shaped (Fig. 4B); 4) some cut through thick sand bodies (which is difficult to explain by desiccation since sand is too coarse and usually not cohesive enough to crack (Lowe, 1975)) (Fig. 4C); 5) some appear suddenly without any obvious connections to the Coconino (Fig. 4D); 6) some penetrate at a downward angle into the Hermit Formation (Fig. 4E); 7) the cracks were closely spaced (Fig. 4G) and not widely separated by many 10's of meters as in modern playa cracks (Fig. 14); 8) microscopy shows that the sand grains in the cracks did not fill the cracks passively because it is tightly packed and some grains are distorted and crushed (Fig. 5F and Table 2), tight packing has been noted in other injectites (Scott et al., 2009); and 9) the sand-filled cracks are associated with sand bodies which appear to be laterally injected sills at Hance Trail and Jumpup Spring and along North and

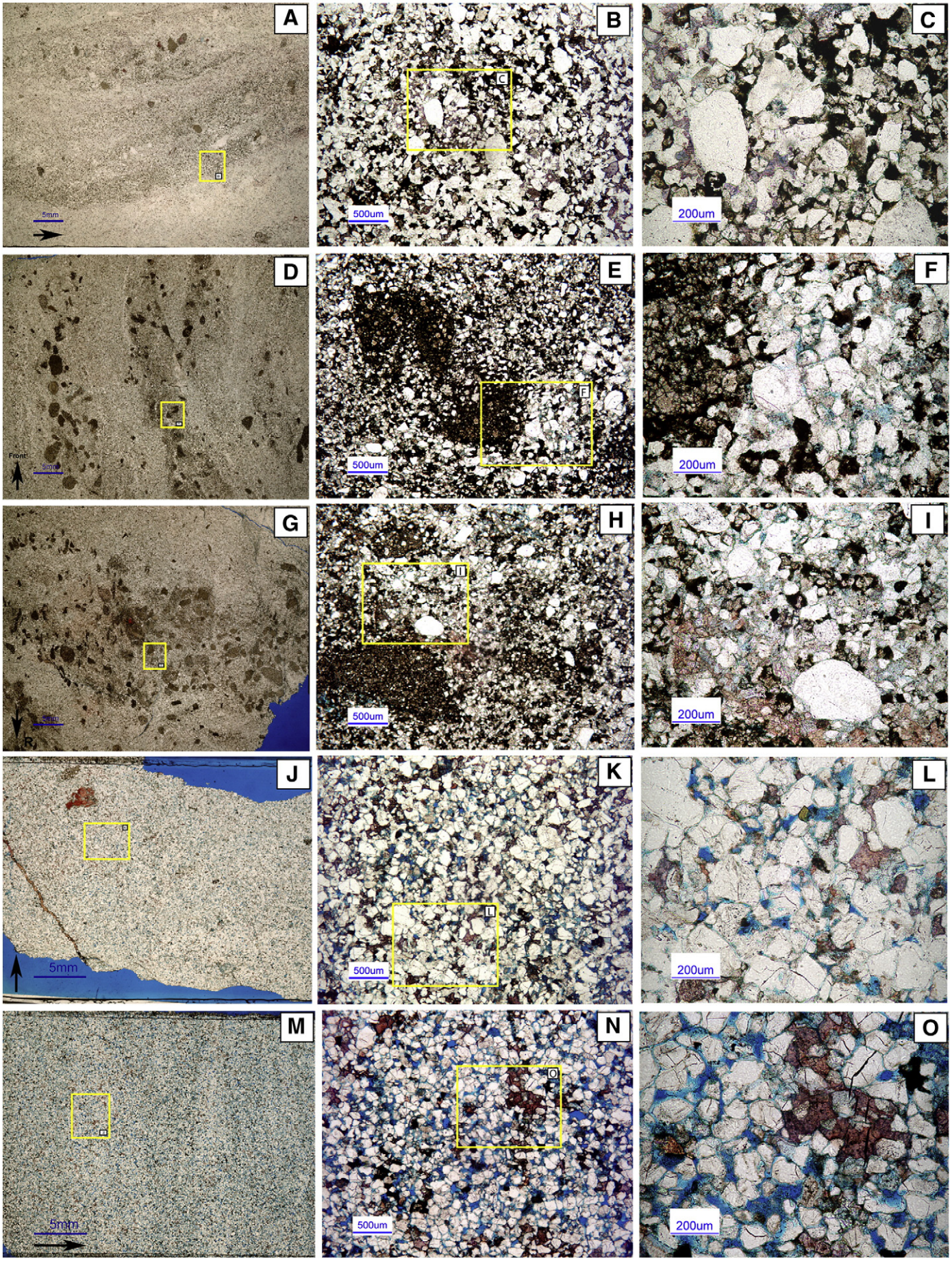

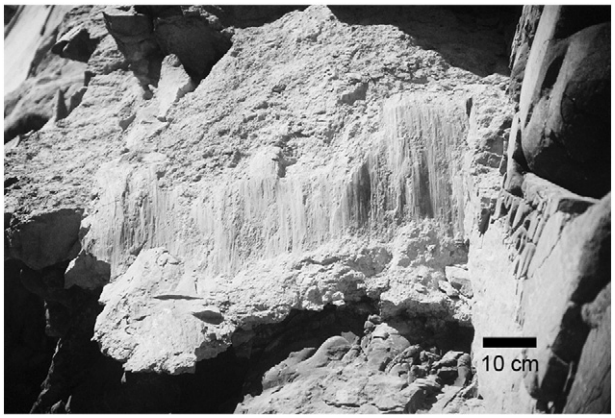

Fig. 6. Slickenside-like features on sand-filled crack BA-2B, Bright Angel Trail. The sand-filled crack is nearly parallel to the rock face. The scale bar is located on a broken area of the crack, showing the entire thickness of the crack. The "slickensides" cut diagonally through the crack from one side of the crack to the other, at a high angle. No obvious offset is present in the Hermit.

South Kaibab Trails. It is difficult to understand how true desiccation cracks or playa cracks could account for such features.

Clastic dikes and injectites have many of the same characteristics as the Grand Canyon cracks: 1) they are commonly massive and have no internal structures (Peterson, 1968; Hiscott, 1979), but 2) some can have flow structures (or banding) within them (Diller, 1889; Jenkins, 1925a; Harms, 1965; Peterson, 1968; Scott et al., 2009), 3) they are most commonly composed of fine to medium grained sand (Harms, 1965; Hiscott, 1979; Jolly and Lonergan, 2002; Obermeier et al., 2002), 4) they are often intimately associated with faulting and tectonic activity (Harms, 1965; Bartholomew et al., 2002; Jolly and Lonergan, 2002), 5) they can be closely spaced (Diller, 1889; Newsom, 1903; Waterston, 1950; Harms, 1965), 6) they can sometimes have zones of shearing within (Harms, 1965; Petit and Laville, 1987; Boehm and Moore, 2002) and 7) they are preferentially oriented (discussed in the next section). The cause of the slickenside-like features found at Bright Angel Trail and Jumpup Spring is uncertain. They may represent "hydroplastic slickensides" as described by Petit and Laville (1987) due to movement in incompletely lithified sediments. Boehm and Moore (2002, p. 156) illustrate "faulting" in a clastic dike, in which the fault does not extend into the surrounding host rock. The "slickensides" and associated "faults" we found at Bright Angel Trail and Jumpup Spring are very similar to what these authors described and pictured.

3.2. Do the cracks have a seismic origin?

Six criteria were developed by Wheeler (2002) to establish whether various soft-sediment structures were formed from seismic or nonseismic processes. Four of these can be directly applied to the Grand Canyon cracks, which suggest that these structures may be ancient seismites. The cracks have a *zoned distribution* about the Bright Angel Fault. They are deepest in the immediate vicinity of the greatest displacement of the fault and dissipate as the distance from the fault increases and as the displacement of the fault decreases (Fig. 2). Crack depth is directly related to the amount of offset and the distance from the fault (i.e., crack depth is related to energy release along the fault). The cracks are similar in *size* to other clastic dikes (Reimnitz and Marshall, 1965; Bourgeois and Johnson, 2001; Stewart et al., 2002). The Bright Angel Fault (and its associated faults) is an appropriate *tectonic setting* for such features to form. Clastic dikes are well known features in various tectonic settings (Harms, 1965; Bartholomew et al., 2002). The Hermit and Coconino are an appropriate *depositional setting* for clastic dikes to form. Dikes can potentially form when fine grained rocks are juxtaposed to water saturated sands that are mobilized during intense tectonic activity. According to Obermeier et al. (2002) liquefaction features form when intense seismic shaking causes the grain-to-grain contacts in water saturated sand to be momentarily lost. Pore water does not have time to escape as strong grain cohesion is lost, allowing pore water to carry the entire weight of the overburden. Massive increases in pore water pressure result, causing water to flow to areas of lower pressure, carrying sand with it. Downward injection of sand can occur as tension develops during faulting and mobilized sand flows downwards, instantaneously filling tension fissures normal to the least direction of stress (Schlische and Ackermann, 1995; Rowe et al., 2002).

Modern studies of large earthquakes have reported many liquefaction features such as sand boils, sand blows and clastic dikes at the surface (Reimnitz and Marshall, 1965; Seed and Idriss, 1982; Holzer, 1998). During these events, liquefied sand is observed to be ejected upward, out of the ground. A few of these studies have examined relatively shallow subsurface features, but none report these features at depth, simply because of the difficulty in observing such structures at depth. However, there seems to be no reason to believe that large earthquakes could initiate *downward* motion of fluidized sand as well. Many examples of downward injected clastic dikes are known from ancient rocks (Cross, 1894; Newsom, 1903; Jenkins, 1925a; Vitanage, 1954; Pratt, 1998a; Matsuda, 2000; Silver and Pogue, 2002; Le Heron and Etienne, 2005). Although on a much larger scale than our sand-filled cracks, Parize et al. (2007) report examples of downwardly injected ("per descensum") dikes from France, that descend 275 m from their source and Netoff (2002) describes some large fluidized pipes of Entrada Sandstone that have been injected downward into the Carmel Formation on the Colorado Plateau. Pressurized water (carrying fluidized sand) can forcefully cause fractures to open (Boehm and Moore, 2002; Jolly and Lonergan, 2002). It is common practice in the petroleum industry to "frac" wells to enhance permeability and production using this very method. Injected fluids exceed the mechanical strength of the rock, inducing fractures into which the fluids travel. Sand-filled artificial fractures can propagate in all directions. Our thin section analysis shows compaction and fracturing of the crack-fill grains, probably caused by this process (look near the center of Fig. 5F, Table 3). Forceful injection of clastic dikes is referred to as "hydrofracturing" or "hydraulic jacking" by Montenat et al. (2007).

Perhaps one of the best evidences for the seismic origin of these cracks is that they have a preferred orientation of about 143° (Fig. 2),

Fig. 5. Petrology of the sand-filled cracks and the Coconino Sandstone above the cracks. Scale bars in the first column are all 5 mm, the second column 500 μm and the third column 200 μm. Each row represents the same rock sample with successive enlargements. Yellow boxes show area and orientation of the enlargement to the right of each figure. A–C: Sand-filled crack SK3 showing flow structure. The thin section is parallel to the front of the crack with the arrow indicating "up." D–F: Sand-filled crack Hn3 showing flow structure. The thin section is parallel to the bottom of the crack with the arrow indicating the direction of "front." E and F show detail of some of the dark clasts (dolomite) within the sand-filled cracks. It is believed these are fragments of Hermit that were entrained, abraded and rounded during crack filling. A large grain in the center of F is fractured showing the forceful emplacement of the material. The fracture is filled with blue epoxy showing the fracturing was present before sample preparation. G–I: Sand-filled crack Hn3 showing flow structure. The thin section is parallel to the front of the crack with the arrow indicating "right." J–L: Sample of Coconino Sandstone from the very base of the unit from the "homogenized zone" about 50 cm to the left of sand-filled crack Hn1 (pictured in Fig. 10). Arrow indicates "up." Red stain and fracture fill on J is calcite. M–O: Sample of cross-bedded Coconino Sandstone from the Hance Trail location, about 2 m above the base of the Coconino. Arrow indicates "up." The many grain fractures in O were caused by sample cutting (they are not filled with blue epoxy). Note that in the thin sections of the sand-filled cracks (A, D and G), large clasts are matrix supported, giving strong evidence of flow processes. Structures like this were found in every one of the cracks sectioned. Very little porosity (blue) is present in any of the tightly packed grains of the cracks showing the sand did not passively fill the cracks. The homogenized zone (J–L) shows increasing porosity, but not as much as the cross-bedded Coconino (M–O). Again, this is evidence of forceful reorganization of the basal Coconino after the initial deposition of the sand grains.

Table 2
Samples collected for thin section analysis from South Kaibab Trail, Arizona (SK). Grand Canyon National Park permit #GRCA-2005-SCI-0011.

Sample	Description and petrology
SK-1	Sand-filled crack SK3, sampled about 2.5 m below Hermit/Coconino contact (Fig. 5A–C). On a macro scale, bedding is vertical and shows strong evidence of flow structures. The quartz sand is moderate to well-cemented, moderately rounded to round. Sand displays a bimodal grain size distribution with the majority of grains falling into the fine sand range (Wentworth scale). Occasional coarse-lower sized grains are observed. Cements include calcite and quartz, with the calcite being dominated by a ferroan variety (stains purple using double carbonate stain). Many quartz grains are corroded, most likely by chemical dissolution associated with calcite cementation. Occasional evidence of compaction is observed as seen in grain suturing and fracturing of quartz grains. Clays present include authigenic illite and kaolinite. Localized porosity is estimated at 1–3% with a drilled plug measured using helium porosimetry yielding a 2.86% porosity value.
SK-2	Sand-filled crack SK5, sampled about 1.5 m below Hermit/Coconino contact. This sample bears a striking resemblance to the previous sample (from sand-filled crack SK3). It is a moderate to well-cemented quartz sand with the main cement being ferroan calcite. Grain size is dominated by moderately-rounded to round fine-upper sand with occasional medium-upper to coarse-lower grains present. Illite and kaolinite are the primary authigenic clays present, with pore-filling kaolinite showing evidence of strong compaction. Kaolinite booklets are both mechanically disturbed and chemically altered. Scanning electron microscopy shows strong quartz cementation. Bent mica flakes also show evidence of strong compaction. Porosity is estimated at 2–5% and varies throughout the zone.
SK-3	Cross-bedded Coconino Sandstone sampled at the very base of Coconino. Moderately cemented quartzose sand. Grain size is bimodal with the dominant size falling into the fine-upper range. Occasional coarse-lower grains are present and are "floating" in the finer matrix. Strong horizontal bedding is partly delineated by grain size, but also (mainly) by dolomitic bands and nearly black organic material. Occasional calcite (non-ferroan) cement is present, but quartz cement is dominant. Quartz cementation is evidenced by sharp euhedral terminations as well as "dust rim" inclusions trapped between the overgrowths and the substrate detrital grains. Grain-sized voids (pore spaces) are commonly seen with some of the grains having been almost completely leached away creating secondary porosity. Some of the pore spaces are partially filled with authigenic kaolinite. It is suspected that rare, precursor feldspars have undergone preferential dissolution and have contributed to the syndiagenetic precipitation of kaolinite, illite and later quartz. Porosity estimated at an average of 10–12%.
SK-4	Cross-bedded Coconino Sandstone, sampled one meter above sample 3. Bedded Quartzose sand with bedding delineated mainly by grain size variation ranging uniformly from fine-upper to medium-lower. Calcite cement is present with ferroan varieties dominating. The sample is moderately cemented by quartz but has not created a well-bonded structure. Remnant feldspar fragments, in relatively open pores, are evidence of precursor grains that have undergone dissolution and have contributed to authigenic kaolinite and illite clays. Original grains are subround to rounded. Estimated porosity ranges between 8% to 14% in this sample.

Table 3
Samples collected for thin section analysis from New Hance Trail, Arizona (NH). Grand Canyon National Park permit #GRCA-2005-SCI-0011.

Sample	Description and petrology
NH-5	Sand-filled crack NH1 (Fig. 10), sampled about 75 cm below the Hermit/Coconino contact. Non-bedded sand with grain size varying between very-fine and fine-upper. Occasional medium-upper grains are seen "floating" in the finer matrix. Localized calcite (non-ferroan) lenses and bands are seen with occasional patches of ferroan calcite randomly distributed throughout the sample. This variation in cementation characteristics is indicative of multiple calcite cementation events. Rare clasts of micro-crystalline dolomite (30–50 μm) are found and are believed to be sourced from the surrounding Hermit Formation. Rare fractures are seen and these are generally filled with mainly non-ferroan calcite. Grain shape varies widely from subangular to rounded. Porosity is estimated at 3–5% with local values up to 8%.
NH-6	Sand-filled crack NH3, sampled just below the Hermit/Coconino contact (See Fig. 5D–I). Quartzose sand with grains varying between very fine to medium-upper. Common rounded dolomite clasts are found in this sample and are thought to be sourced from the surrounding Hermit Formation. Calcite cement, both ferroan and non-ferroan varieties, is commonly present. Horizontal bedding is noticeably absent. While vertical flow structures appear to be common as evidenced by clast distribution in the sand matrix, the dolomite clasts appear to contour the crack wall. Porosity is estimated at 4–6%.
NH-7	Structureless sandstone at very base of Coconino (Fig. 5 J–L), sampled about 50 cm to the left of crack Hn1 (Fig. 10). Quartzose sand, poorly to moderately sorted. Grains are subangular to subrounded in form. Calcite cement is commonly ferroan as evidenced by the purple staining however, non-ferroan calcite is also present locally and as fracture fills. Grain size is fine-upper to medium lower. Bedding is virtually absent in this sample. Numerous quartz grains show evidence of edge corrosion where they are in contact with calcite cement. Kaolinite is commonly found as pore linings and pore-fills. Authigenic illite is also present in minor amounts. Rare quartz cement is seen as clean euhedral crystals underlain by dust rims. Porosity is estimated to be between 7 to 9%.
NH-8	Cross-bedded Coconino Sandstone, sampled about 2 m above the Hermit/Coconino contact (Fig. 5M–O). Moderately-sorted sand. Grains are subangular to subrounded. Bedding is weak with bedding defined primarily by open porosity versus tighter zones of more closely packed sand grains. Ferroan calcite is common in this zone as well. Quartz cement is common. One glauconite pellet found within the sample, similar to those found in sub-aqueous depositional environments. Porosity is mainly primary with some secondary porosity in evidence. What clearly appears to be a glauconite pellet is seen in this sample. Secondary porosity is evident in this sample. Authigenic kaolinite is common in the sample with authigenic illite also commonly seen. Porosity ranges from 14 to 16%.

or a northwestern–southeastern orientation. This is approximately perpendicular to the Bright Angel-Eminence Fault Zones and parallels other northwest trending faults and fractures of the area (Huntoon and Sears, 1975; Brumbaugh 2005). When clastic dikes form in association with normal faults, they usually develop parallel to the fault, from tension fractures opening and instantaneously filling. However, the sand-filled cracks described here are perpendicular to the Bright Angel Fault. It seems there is some relationship between the cracks and the fault because of the zoned distribution of the cracks

Fig. 7. A large lateral sand body within the Hermit Formation along New Hance Trail.

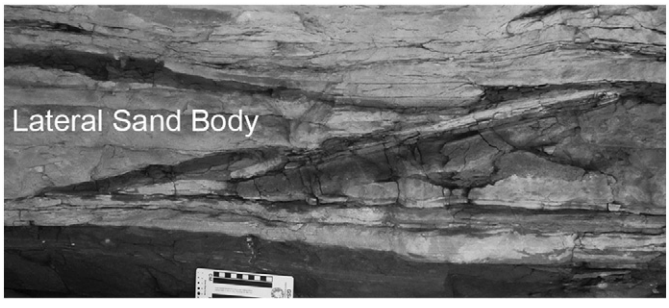

Fig. 8. The distal end of a lateral sand body along New Hance Trail. Note how the sand body has spread apart the layers of the Hermit Formation. Scale bar is 10 cm long.

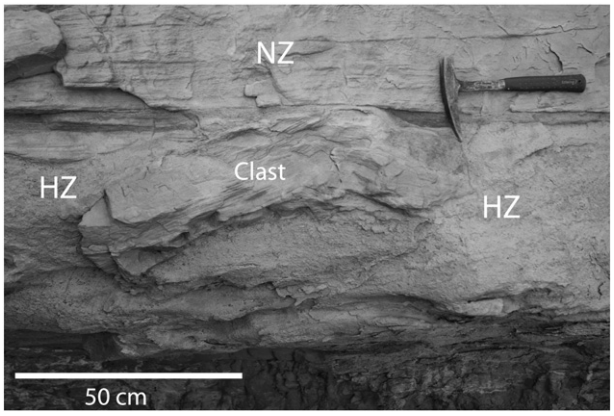

Fig. 9. The homogenized zone (HZ) containing a large bedded clast of Coconino along the South Fork of Rock Canyon, Arizona. The Coconino/Hermit Contact is near the bottom of the photo. The homogenized zone rests directly on the Hermit. A normally bedded zone of Coconino (NZ) begins just below the rock hammer handle. Notice how the homogenized zone intrudes above the clast of bedded Coconino on both ends of the clast.

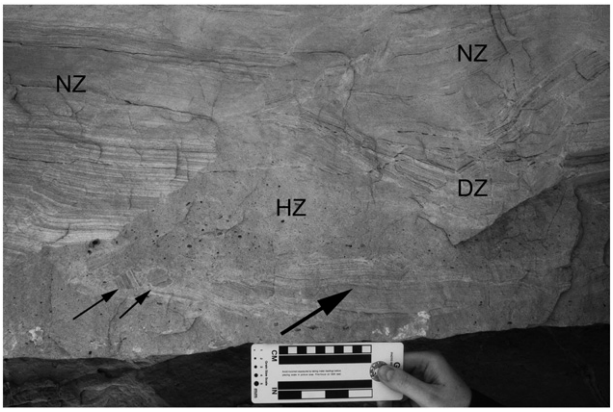

Fig. 11. Part of the homogenized (structureless) zone (HZ) at the bottom of the Coconino, New Hance Trail. The zone is up to 2 m thick and sometimes has a distorted zone (DZ) above it that grades into a normally cross-bedded Coconino zone (NZ). Occasionally, layered clasts of bedded Coconino can be found within (indicated by arrows). Two smaller clasts, with bedding askew to that of the Coconino, are shown by the smaller black arrows. The larger black arrow is in the middle of a slab-like clast in excess of 25 cm long. Note the sharp boundary between the homogenized zone and normal zone on the left.

around the fault, and their occurrence only in the vicinity of the fault (i.e., none are found outside the Grand Canyon area). We speculate that the perpendicular nature of the cracks might be due to the unusual "reverse drag" motion of the Bright Angel Fault (Huntoon and Sears, 1975, p. 470) perhaps causing minor tension, parallel to the fault. Another explanation might be that filling of the cracks was influenced by the reactivation of pre-existing, Precambrian-age northeast trending fractures, which were pulled open in a system of tension very similar to what is observed today (Brumbaugh, 2005). A precise reason for sand-filled crack orientation and what their relationship is to the fault may not become apparent without further detailed structural analysis.

3.3. Significance of the homogenized sand at the base of the Coconino

Petrographic observation of the crack-fill material and the homogenized zone at the base of the Coconino show these units have much lower porosities than the bedded portions of the Coconino (compare Figs. 5C, F and I with Figs. 5L and O). Porosities range from 8–16% in the bedded Coconino, 7–9% in the structureless zone, and from 1–8% in the cracks (Tables 2, 3). Reorientation and tighter repacking of sand grains commonly follows a liquefaction event (Owen, 1987; Scott et al., 2009). Lower porosities in the sand-filled cracks and the homogenized zone compared to the Coconino above the homogenized zone, support the hypothesis that the structureless zone became homogenized during a liquefaction event. Homogenization of bedded sediments is typical of liquefaction during seismic activity (Lowe, 1975, 1976; Matsuda, 2000; Moretti, 2000; Moretti and Tropeano, 2002; Onasch and Kahle, 2002). Decreased porosities have been noted in other sandstones that have been injected, when compared to the primary sands from which they were sourced (Lonergan et al., 2007).

One of the most notable characteristics of the Coconino is that it has distinct laminated bedding throughout. Hance Trail, Grandview Trail and the South Fork of Rock Canyon are the first known locations reported of a different bedding style within the Coconino. Some may suggest these homogenized zones may be due to slumping or avalanching of aeolian dunes. This hypothesis was considered, but avalanche and slump structures are quite distinctive and do not result in the structureless sand like that found in the homogenized zones (McKee et al., 1971; McKee and Bigarella, 1972; Hunter, 1977). The features in the homogenized zones are not similar to the large scale soft sediment deformation features reported from the Navajo Sandstone (Doe and Dott, 1980) either. Structureless sand can be found in modern aeolian settings, but McKee and Tibbitts (1964) only report it from an interdunal area, not from within active dunes. McKee and Bigarella (1972) reported rotated breccia clasts that formed from slumping of wet sand dunes along the Brazilian coast. However, these

Fig. 10. A sand-filled crack at the base of the Coconino Sandstone along Hance Trail (crack Hn1). Here, the base of the Coconino is homogenized, showing no bedding. 10 cm scale bar in lower right corner.

Fig. 12. Small load cast-like structures at the base of the Coconino Sandstone, New Hance Trail. Note the small associated sand-filled cracks at the Hermit/Coconino contact. Scale bar (cm) is near the front of the photo. There is approximately 1.0 of depth in the picture.

Table 4
X ray diffraction analysis and average clastic particle size of the Hermit Formation. For comparison, Lucerne Dry Lake (LDL) sediments were also analyzed; a dry lake which exhibits large playa cracks.

Sample number	Cracks present?	Average particle size (μm)[a]	Total clay % <5 μm by mass	Weight fraction of clay minerals present (%) in bulk powder	Volume fraction of clay minerals present (%) in bulk powder	Volume fraction of illite present (%) in clay smear (<5 μm)	Volume fraction of kaolinite present (%) in clay smear (<5 μm)
AC-1	No	41.3	3.5	2	2	61	21
AP-7	No	38.5	3.1	0	0	60	16
HC-1	No	44.4	3.3	0	0	72	15
JUS-3	Yes	41.3	2.9	0	0	52	21
SFRC-1	Yes	43.7	5.0	2	2	75	12
WC-1	No	36.1	3.9	3	3	46	40
WSC-20	Yes	44.4	5.5	0	0	64	23
LDL-1	Yes		25.9	9	8	58	5

[a] Determined by measuring the long axis of 75 quartz grains (the dominant mineral) at 200x in a single random microscope field of view with Nikon NIS Elements BR software. These quartz particles make up about 90% of the rock by volume.

were also associated with normal faulting and folding within the dunes; no evidence of this occurs anywhere in the locations where we found the homogenized zones.

The homogenized zone, distorted zone and normal cross-bedded zone of the Coconino grade into one another in some places (right center of Fig. 11). But in other places the contact is sharp between the homogenized zone and the cross-bedded Coconino (Fig. 9 and left center of Fig. 11). This likely indicates substratal deformation and flow. Furthermore, the homogenized zone occurs horizontally, for up to 40 m along the base of the Coconino. It is not found anywhere higher in the section as might be expected if the loss of structure was produced by aeolian processes. The homogenized zone, containing the bedded clasts of Coconino, has elements of the intrastratal rip-down clasts described by Chough and Chun (1988) and the intrastratal flow structures described by Kawakami and Kawamura (2002). Scott et al. (2009) found a bedded mudstone clast within the injectite they studied, which is similar to the clasts we found. It is proposed our sandstone clast breccias resulted from substratal liquefaction and subsequent flow of the basal Coconino during the same seismic event that produced the sand-filled cracks and lateral sand bodies. The homogenized zone is integrally associated with the cracks and load casts (Figs. 4E, 10 and 12) and is further evidence that liquefied Coconino was injected downward into the cracks. We think it is significant that loading structures occur along Hance Trail (Fig. 12). Hildebrandt and Egenhoff (2007) report similar loading structures in association with clastic dikes and structureless sandstones. They suggest seismic activity was responsible for loading features, liquefied sand and clastic dikes found in their study area. All of the same features are found along Hance Trail.

We think that many of the sand-filled cracks may not have been injected directly downward, but more or less at a downward angle (as shown in Fig. 4E). Some dikes may have traveled significant horizontal distances from their source area. It is possible for sand injectites to travel laterally for 100's of meters or more (Hurst and Cartwright, 2007). This may be why distorted Coconino is not commonly found above the sand-filled cracks. One of the thin sections made from a crack along Hance Trail (NH 1, shown in Fig. 10) showed the sand was flowing laterally, not vertically. The sample contained matrix supported Hermit clasts that were nearly horizontal and contained flow structures and banding similar to those shown in Fig. 5A, D and G. Sand which traveled laterally can help us understand how some cracks appear not to be directly connected to the Coconino, why some cracks taper upwards and why some cracks are "U" shaped (Fig. 4A, B, D).

Table 5
Particle size distribution of sediments from 11 fissured playas studied by Neal et al. (1968).

Playa	% Particle size			
	<5 μm	5–40 μm	40–120 μm	>120 μm
Red Lake	55	17	28	0
Indian Springs	30	34	36	0
Ivanpah	56	6	38	0
Bicycle	45	14	40	1
North Panamint	32	15	43	0
Rosamond	71	4	25	0
Rogers	65	3	30	2
Coyote	53	10	32	5
Animas	65	7	28	0
Alvord	35	20	32	13
Eldorado	49	9	40	2
Average	51	13	34	2

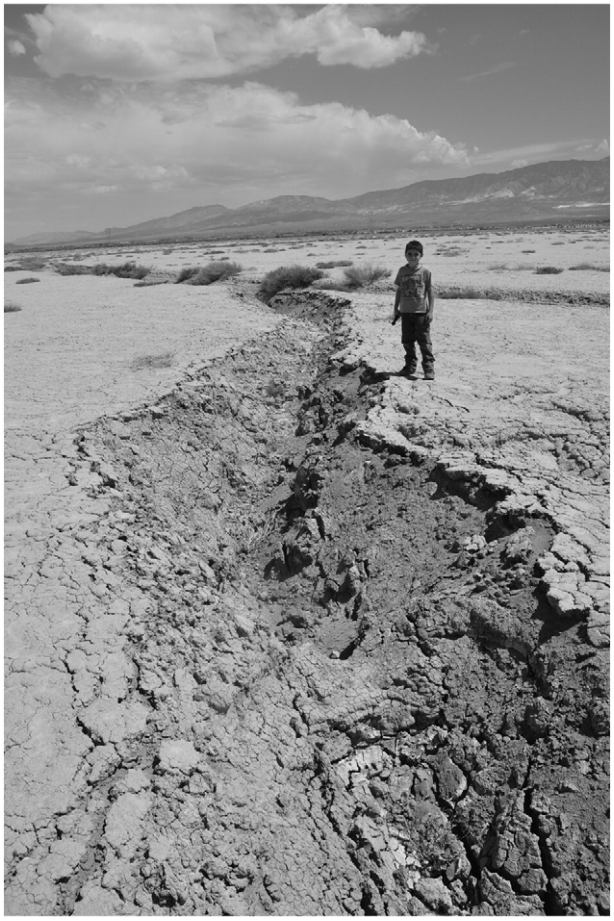

Fig. 13. A large desiccation playa crack, filled with sloughed in material from the sides of the crack. Lucerne Lake, California. Note smaller desiccation cracks that occur on the playa surface.

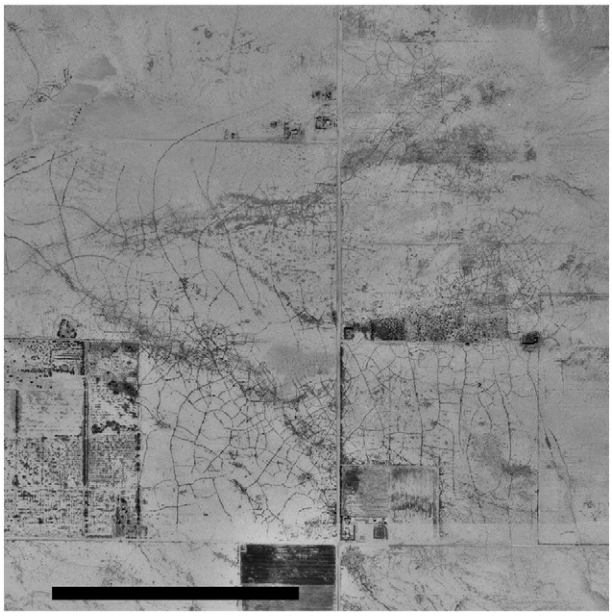

Fig. 14. Aerial view of Lucerne Lake, California, showing large polygonal playa cracks. Scale bar is 1 km. Photo downloaded from Topozone.com.

3.4. Are some of the sand-filled cracks desiccation cracks?

We do not believe that any of the sand-filled cracks found at the bottom of the Coconino Sandstone are desiccation cracks. We understand why the cracks have been called desiccation cracks in the past; they fit well within paleoenvironmental interpretations of the Hermit and Coconino. Additionally, many of them are small and wedge shaped. However, in all the outcrops we visited throughout the Grand Canyon region, the cracks consistently exhibited the same features. Never did any of the cracks show macroscopic horizontal bedding as would be expected if the cracks were open to air and were filled by windblown or fluvial processes. Surely, if this is how they were filled, a great majority of the cracks would show clear horizontal bedding. William Morris Davis (1889) made a similar logical conclusion in discussing clastic dikes reported by Diller (1889). He even gave an example of some open air cracks that had been filled with transverse layering. Some desiccation cracks may be present in our study area, but we haven't found any reasonable candidates.

3.5. Timing of sand-filled crack formation

Evidence at the Hermit–Coconino contact suggests the sand-filled cracks formed before the Hermit and Coconino were fully lithified. Smaller sand-filled cracks often exhibit ptygmatic folds indicating differential compaction of Hermit compared to the sand-filled cracks. Larger cracks are often not folded; perhaps because they acted like semi-rigid "struts" during compaction of the Hermit. The load cast-like features associated with the sand-filled cracks along Hance Trail also suggest the Hermit was somewhat unlithified during crack filling. It is possible that some of the upturned ends of the lateral sand bodies within the Hermit are also deformed as a result of differential compaction. Small bits of Hermit within the sand-filled cracks show the Hermit may have been at least partially lithified.

Since the cracks have a zoned distribution about the Bright Angel Fault, it appears movement along the fault caused liquefaction and injection of the dikes. The fault was active during the Precambrian, possibly only for a brief time between the deposition of the Redwall Limestone (Mississippian) and the lower Supai Group (Pennsylvanian), and then during Laramide deformation of the area (Huntoon and Sears, 1975; Shoemaker et al., 1978) during the Miocene or Pliocene. These cited authors agree that the fault was relatively inactive between the Precambrian and the Laramide deformation.

A problem with no readily apparent solution is that it appears the basal Coconino was water saturated and unlithified (or only partially lithified) at the time of Laramide faulting which we suspect caused dike intrusion. It is unlikely the Coconino could have remained uncemented in excess of 250 million years. Solutions to this dilemma might include removal of the basal Coconino cement just prior to Laramide faulting; or sufficient and previously unknown movement of the Bright Angel Fault shortly after deposition of the basal Coconino. We welcome further structural analysis on the Bright Angel Fault, considering the new patterns we have established, so the timing and orientation of the sand-filled cracks can be better understood.

4. Conclusion

The previous interpretation that the sand-filled cracks at the base of the Coconino are desiccation cracks is problematic. They lack features common to desiccation and playa cracks, especially in regards to crack width, crack spacing and crack fill. None of the cracks show horizontal bedding as would be expected if these cracks filled due to the Coconino dunes blowing in over the mud cracked Hermit floodplain. Furthermore, it appears the Hermit Formation lacks the appropriate clay minerals and clay-sized particles to crack via desiccation. Instead, evidence suggests the basal Coconino was water saturated and underwent liquefaction during an ancient seismic episode, perhaps along the Bright Angel Fault. The most conclusive evidence includes a zoned crack depth distribution; preferred orientation of the sand-filled cracks; widespread homogenized zones containing brecciated clasts of bedded Coconino attached to sand-filled cracks; vertical flow structures within sand-filled cracks; and the association of the sand-filled cracks with lateral sand bodies near the top of the Hermit. Thin section studies of the crack fills, homogenized zones, and bedded portions of the Coconino support the hypothesis that the sand-filled cracks are clastic dikes and that the lateral sand bodies may be clastic sills. Particle size analysis, XRD studies and clay mineral analysis show the Hermit does not have the appropriate lithology to crack via desiccation. Although we believe the data we have presented here clearly identifies these features as sand injectites, further structural study is needed to determine the full extent and timing of this phenomenon in the Grand Canyon region. We welcome further structural analysis on the Bright Angel Fault in consideration of the new patterns we have found. Caution is warranted when interpreting all types of sand-filled cracks, because many are similar in outside appearance, but can vary in internal structure. Paleoenvironmental presuppositions can lead to erroneous interpretations of various features and might cause one to overlook important data.

Acknowledgements

We thank Cedarville University and Calgary Rock and Materials Services Inc. and some private donors for logistical help and funding. Grand Canyon National Park allowed samples to be collected with permit #GRCA-2005-SCI-0011. We are grateful to those who helped with field work and who carefully reviewed and improved our manuscript.

References

Abbott, L., Cook, T., 2004. Hiking the Grand Canyon's Geology. Mountaineers Books, Seattle, WA.

Astin, T.R., Rogers, D.A., 1991. "Subaqueous shrinkage cracks" in the Devonian of Scotland reinterpreted. Journal of Sedimentary Petrology 61, 850–859.

Barclay, W.J., Glover, B.W., Mendum, J.R., 1993. "Subaqueous shrinkage cracks" in the Devonian of Scotland reinterpreted—discussion. Journal of Sedimentary Petrology 63, 564–565.

Bartholomew, M.J., Brodie, B.M., Willoughby, R.H., Lewis, S.E., Syms, F.H., 2002. Mid-Tertiary Paleoseismites: Syndepositional Features and Section Restoration Used to indicate Paleoseismicity, Atlantic Coastal Plain, South Carolina and Georgia. In: Ettensohn, F.R., Rast, N., Brett, C.E. (Eds.), Ancient Seismites. : Special Paper, vol. 359. Geological Society of America, Boulder, CO, pp. 63–74.

Basma, A.A., Al-Homoud, A.S., Malkawi, A.I.H., Al-Bashabsheh, M.A., 1996. Swelling-shrikage behavior of natural expansive clays. Applied Clay Science 11, 211–227.
Blakey, R.C., 1990. Stratigraphy and geologic history of Pennsylvanian and Permian rocks, Mogollon Rim region, central Arizona and vicinity. Geological Society of America Bulletin 102, 1189–1217.
Blakey, R.C., 1996. Permian Eolian Deposits, Sequences, and Sequence Boundaries, Colorado Plateau. In: Longman, M.W., Sonnenfeld, M.D. (Eds.), Paleozoic Systems of the Rocky Mountain Region. Rocky Mountain Section SEPM, Denver, CO, pp. 405–426.
Boehm, A., Moore, J.C., 2002. Fluidized sandstone intrusions as an indicator of paleostress orientation, Santa Cruz, California. Geofluids 2, 147–161.
Bourgeois, J., Johnson, S.Y., 2001. Geologic evidence of earthquakes at the Snohomish Delta, Washington, in the past 1200 yr. Geological Society of America Bulletin 113, 482–494.
Brumbaugh, D.S., 2005. Active faulting and seismicity in a prefactured terrane: Grand Canyon, Arizona. Bulletin of the Seismological Society of America 95, 1561–1566.
Chough, S.K., Chun, S.S., 1988. Intrastratal rip-down clasts, Late Cretaceous Uhangri Formation, southwest Korea. Journal of Sedimentary Petrology 58, 530–533.
Cowan, C.A., James, N.P., 1992. Diastasis Cracks: mechanically generated synaeresis-like cracks in Upper Cambrian shallow water oolite and ribbon carbonates. Sedimentology 39, 1101–1118.
Cross, C.W., 1894. Intrusive sandstone dikes in granite. Bulletin of the Geological Society of America 5, 225–230.
Davis, W.M., 1889. Discussion [of Diller, 1889]. Bulletin of the Geological Society of America 1, 442.
Diller, J.S., 1889. Sandstone dikes. Bulletin of the Geological Society of America 1, 411–442.
Doe, T.W., Dott, R.H., 1980. Genetic significance of deformed cross bedding– with examples from the Navajo and Weber Sandstones, Utah. Journal of Sedimentary Petrology 50, 793–812.
Donovan, R.N., Foster, R.J., 1972. Subaqueous shrinkage cracks from the Caithness Flagstone Series (Middle Devonian) of northeast Scotland. Journal of Sedimentary Petrology 42, 309–317.
Harianto, T., Hayashi, S., Du, Y.-J., 2008. Effects of fiber additives on the desiccation crack behavior of the compacted Akaboku Soil as a material for landfill cover barrier. Water, Air, and Soil Pollution 194, 141–149.
Harms, J.C., 1965. Sandstone dikes in relation to Laramide faults and stress distribution in the southern Front Range, Colorado. Geological Society of America Bulletin 76, 981–1002.
Harris, R.C., 2004. Giant desiccation cracks in Arizona. Arizona Geology 34 (2), 1–4.
Hildebrandt, C., Egenhoff, S., 2007. Shallow-marine massive sandstone sheets as indicators of paleoseismic liquefaction — an example from the Ordovician shelf of Central Boliva. Sedimentary Geology 202, 581–595.
Hiscott, R.N., 1979. Clastic sills and dikes associated with deep-water sandstones, Tourelle Formation, Ordovician, Quebec. Journal of Sedimentary Petrology 49, 1–10.
Holzer, T.L., 1998. The Loma Prieta, California, Earthquake of October 17. 1989—liquefaction. U.S. Geological Survey Professional Paper 1551-B, pp. 1–314.
Hunter, R.E., 1977. Basic types of stratification in small eolian dunes. Sedimentology 24, 361–387.
Huntoon, P.W., Sears, J.W., 1975. Bright angel and eminence faults, eastern Grand Canyon, Arizona. Geological Society of America Bulletin 86, 465–472.
Huntoon, P.W., Billingsley, G.H., Sears, J.W., Bradley, R.I., Karlstrom, K.E., Williams, M.L., Hawkins, D., Breed, W.J., Ford, T.D., Clark, M.D., Babcock, R.S., Brown, E.H., 1996. Geologic Map of the Eastern Part of the Grand Canyon National Park, Arizona. Grand Canyon Association, Grand Canyon, AZ.
Hurst, A., Cartwright, J., 2007. Relevance of Sand Injectites to Hydrocarbon Exploration and Production. In: Hurst, A., Cartwright, J. (Eds.), Sand Injectites: Implications for Hydrocarbon Exploration and Production: AAPG Memoir, vol. 87, pp. 1–19.
Jenkins, O.P., 1925a. Clastic dikes of eastern Washington and their geological significance. American Journal of Science (5th Series) 10, 234–246.
Jenkins, O.P., 1925b. Mechanics of clastic dike intrusion. Engineering and Mining Journal-Press 120, 12.
Jolly, R.J.H., Lonergan, L., 2002. Mechanisms and controls on the formation of sand intrusions. Journal of the Geological Society London 159, 605–617.
Kawakami, G., Kawamura, M., 2002. Sediment flow and deformation (SFD) layers: evidence for intrastratal flow in laminated muddy sediments of the Triassic Osawa Formation, northwest Japan. Journal of Sedimentary Research 72, 171–181.
Lang, W.B., 1943. Gigantic drying cracks in Animas Valley, New Mexico. Science 98, 583–584.
Le Heron, D.P., Etienne, J.L., 2005. A complex subglacial clastic dyke swarm, Sólheimajökull, southern Iceland. Sedimentary Geology 181, 25–37.
Lonergan, L., Borlandeli, C., Taylor, A., Quine, M., Flanagan, K., 2007. Three-Dimensional Geometry of Sandstone Injection Complexes in the Gryphon Field, United Kingdom, North Sea. In: Hurst, A., Cartwright, J. (Eds.), Sand Injectites: Implications for Hydrocarbon Exploration and Production: AAPG Memoir, vol. 87, pp. 103–112.
Lowe, D.R., 1975. Water escape structures in coarse-grained sediments. Sedimentology 22, 157–204.
Lowe, D.R., 1976. Subaqueous liquefied and fluidized sediment flows and their deposits. Sedimentology 23, 285–308.
Matsuda, J.-I., 2000. Seismic deformation structures of the post-2300 a BP muddy sediments in Kawachi lowland plain, Osaka, Japan. Sedimentary Geology 135, 99–116.
McKee, E.D., 1934. The Coconino Sandstone—its history and origin. Papers Concerning the Palaeontology of California, Arizona, and Idaho. Carnegie Institution, Washington D.C, pp. 77–115.
McKee, E.D., 1979. Ancient sandstones considered to be eolian. In: McKee, E.D. (Ed.), A Study of Global Sand Seas: U.S. Geological Survey Professional Paper, 1052, pp. 187–238.
McKee, E.D., Bigarella, J.J., 1972. Deformational structures in Brazilian coastal dunes. Journal of Sedimentary Petrology 42, 670–681.
McKee, E.D., Tibbitts Jr., G.G., 1964. Primary structures of a seif dune and associated deposits in Libya. Journal of Sedimentary Petrology 34, 5–17.
McKee, E.D., Douglass, J.R., Rittenhouse, S., 1971. Deformation of lee-side laminae in eolian dunes. Geological Society of America Bulletin 82, 359–378.
Montenat, C., Barrier, P., d'Estevou, P.O., Hibsch, C., 2007. Seismites: an attempt at critical analysis and classification. Sedimentary Geology 196, 5–30.
Moretti, M., 2000. Soft-sediment deformation structures interpreted as seismites in middle-late Pleistocene Aeolian deposits (Apulian foreland, southern Italy). Sedimentary Geology 135, 167–179.
Moretti, M., Tropeano, M., 2002. Late Pleistocene Soft-Sediment Deformation Structures Interpreted as Seismites in Paralic Deposits in the City of Bari (Apulian foreland, southern Italy). In: Ettensohn, F.R., Rast, N., Brett, C.E. (Eds.), Ancient Seismites. : Special Paper, vol. 359. Geological Society of America, Boulder, CO, pp. 75–85.
Neal, J.T., Langer, A.M., Kerr, P.F., 1968. Giant desiccation polygons of Great Basin playas. Geological Society of America Bulletin 79, 69–90.
Netoff, D., 2002. Seismogenically induced fluidization of Jurassic erg sands, south-central Utah. Sedimentology 49, 65–80.
Newsom, J.F., 1903. Clastic dikes. Bulletin of the Geological Society of America 14, 227–268.
Noble, L.F., 1922. A section of the Paleozoic formations of the Grand Canyon at Bass Trail. U.S. Geological Survey Professional Paper 131-B, pp. 23–73.
Obermeier, S.F., Pond, E.C., Olson, S.M., Green, R.A., 2002. Paleoliquefaction Studies in Continental Settings. In: Ettensohn, F.R., Rast, N., Brett, C.E. (Eds.), Ancient Seismites. : Special Paper, vol. 359. Geological Society of America, Boulder, CO, pp. 13–27.
Onasch, C.M., Kahle, C.F., 2002. Seismically Induced Soft-Sediment Deformation in Some Silurian Carbonates, Eastern U.S. Midcontinent. In: Ettensohn, F.R., Rast, N., Brett, C.E. (Eds.), Ancient Seismites. : Special Paper, vol. 359. Geological Society of America, Boulder, CO, pp. 165–176.
Owen, G., 1987. Deformation Processes in Unconsolidated Sands. In: Jones, M.E., Preston, R.M.F. (Eds.), Deformation of Sediments and Sedimentary Rocks. : Geological Society Special Publication, vol. 29. Blackwell Scientific Publications, Oxford, pp. 11–24.
Parize, O., Beaudoin, B., Champanhet, J.-M., Friès, G., Imbert, P., Labourdette, R., Paternoster, B., Rubino, J.-L., Schneider, F., 2007. A Methodological Approach to Clastic Injectites: From Field Analysis to Seismic Modeling — Examples of the Vocontian Aptian and Albian Injectites (Southeast France). In: Hurst, A., Cartwright, J. (Eds.), Sand Injectites: Implications for Hydrocarbon Exploration and Production: AAPG Memoir, 87, pp. 173–183.
Peterson, G.L., 1968. Flow structures in sandstone dikes. Sedimentary Geology 2, 177–190.
Petit, J.-P., Laville, E., 1987. Morphology and Microstructures of Hydroplastic Slickensides in Sandstone. In: Jones, M.E., Preston, R.M.F. (Eds.), Deformation of Sediments and Sedimentary Rocks. : Geological Society Special Publication, vol. 29. Blackwell Scientific Publications, Oxford, pp. 107–121.
Plummer, P.S., Gostin, V.A., 1981. Shrinkage cracks: desiccation or synaeresis? Journal of Sedimentary Petrology 51, 1147–1156.
Pratt, B.R., 1998a. Molar-tooth structure in Proterozoic carbonate rocks: origin from synsedimentary earthquakes, and implications for the nature and evolution of basins and marine sediment. Geological Society of America Bulletin 110, 1028–1045.
Pratt, B.R., 1998b. Syneresis cracks: subaqueous shrinkage in argillaceous sediments caused by earthquake-induced dewatering. Sedimentary Geology 117, 1–10.
Reimnitz, E., Marshall, N.F., 1965. Effects of the Alaska earthquake and tsunami on recent deltaic sediments. Journal of Geophysical Research 70, 2363–2376.
Rowe, C.A., Mustard, P.S., Mahoney, J.B., Katnick, D.C., 2002. Oriented clastic dike swarms as indicators of paleoslope? An example from the upper Cretaceous Nanaimo Group, Canada. Journal of Sedimentary Research 72, 192–200.
Schlische, R.W., Ackermann, R.V., 1995. Kinematic significance of sediment-filled fissures in the North Mountain Basalt, Fundy Rift Basin, Nova Scotia, Canada. Journal of Structural Geology 17, 987–996.
Scott, A., Vigorito, M., Hurst, A., 2009. The process of sand injection: internal structures and relationships with host strata (Yellowbank Creek Injectite Complex, California, U.S.A.). Journal of Sedimentary Research 79, 568–583.
Seed, H.B., Idriss, I.M., 1982. Ground Motions and Soil Liquefaction during Earthquakes. Earthquake Engineering Research Institute, Berkeley, CA.
Shoemaker, E.M., Squires, R.L., Abrams, M.J., 1978. Bright Angel and Mesa Butte fault systems of northern Arizona. In: Smith, R.B., Eaton, G.P. (Eds.), Cenozoic Tectonics and Regional Geophysics of the Western Cordillera: Geological Society of America Memoir, vol. 152, pp. 341–367.
Silver, M.H., Pogue, K.R., 2002. Analysis of plan-view geometry of clastic dike networks in Missoula flood slackwater sediments (touchet beds), southeastern Washington. Geological Society of America Abstracts with Programs 34, 24.
Stewart, K.G., Dennison, J.M., Bartholomew, M.J., 2002. Late Mississippian paleoseismites from southeastern West Virginia and southwestern Virginia. In: Ettensohn, F.R., Rast, N., Brett, C.E. (Eds.), Ancient Seismites. : Special Paper, vol. 359. Geological Society of America, Boulder, CO, pp. 127–144.
Vitanage, P.W., 1954. Sandstone dikes in the South Platte area, Colorado. Journal of Geology 62, 493–500.
Waterston, C.D., 1950. Note on the sandstone injections of Eathie Haven, Cromarty. Geological Magazine 87, 133–139.

Wheeler, R.L., 2002. Distinguishing Seismic from Nonseismic Soft-Sediment Structures: Criteria from Seismic-Hazard Analysis. In: Ettensohn, F.R., Rast, N., Brett, C.E. (Eds.), Ancient Seismites. : Special Paper, vol. 359. The Geological Society of America, Boulder, CO, pp. 1–11.

White, D., 1929. Flora of the Hermit Shale, Grand Canyon, Arizona. Carnegie Institution of Washington, Washington D.C. Publication 405.

Wilden, R., Mabey, D.R., 1961. Giant desiccation fissures on the Black Rock and Smoke Creek Deserts, Nevada. Science 133, 1359–1360.

Yassoglou, N., Kosmas, C.S., Moustakas, N., Tzianis, E., Danalatos, N.G., 1994. Cracking in recent alluvial soils as related to easily determined soil properties. Geoderma 63, 289–298.

Yesiller, N., Miller, C.J., Inci, G., Yaldo, K., 2000. Desiccation and cracking behavior of three compacted landfill liner soils. Engineering Geology 57, 105–121.